DEVELOPMENT OF A GAN-FET-BASED FAST CORRECTOR MAGNET POWER SUPPLY FOR THE TPS

B. S. Wang, K. B. Liu and Y. S. Wong
NSRRC, Hsinchu 300092, Taiwan

Abstract

A modular GaN-FET-based fast corrector magnet power supply has been developed for the Taiwan Photon Source (TPS). The high switching speed of GaN devices enables a significant increase in the output current bandwidth, which improves the response of the fast orbit feedback (FOFB) system and enhances the overall beam stability and photon beam quality of TPS. In the existing FOFB system, the operating current of the corrector magnet power supply is within ±5 A. The developed power supply provides a maximum output current of ±5 A and achieves improved current resolution by optimizing the internal turn ratio of the DC current transformer (DCCT). A digital control architecture is implemented, integrating an ADC interface, interlock protection, and a PI controller, and is fully compatible with the TPS control system. With a switching frequency of 250 kHz, the proposed power supply achieves a current control bandwidth of approximately 9 kHz, providing a significant improvement over the existing system.

INTRODUCTION

The TPS has achieved excellent beam quality and stable operation over the past decade. To further enhance beam stability and meet increasing demands for high-precision experiments, upgrades of accelerator subsystems are necessary, particularly to improve the bandwidth of the FOFB system for suppressing rapid orbit disturbances.

The TPS storage ring consists of 24 sectors, each equipped with bending, quadrupole, and sextupole magnets, as well as seven beam position monitors (BPMs) as shown in Fig.1 [1].

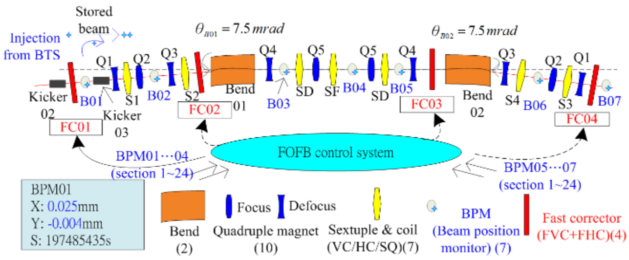

Figure 1: Distribution of BPMs and Fast CMPS.

The FOFB system relies on fast corrector magnets driven by power supplies with limited bandwidth (≈1.6 kHz small-signal at 40 kHz switching) [2]. To improve FOFB performance, a higher-bandwidth, higher-resolution digital fast corrector magnet power supply (DFCMPS) was developed. The design employs a digital control architecture, GaN FETs in a modular full-bridge topology (250 kHz switching), and LEM ITN-12-P DCCT current feedback, achieving ±5 A full-scale resolution while maintaining compatibility with existing TPS infrastructure. Experimental results demonstrate enhanced bandwidth and current stability, validating the proposed system.

DESIGN OF THE DFCMPS

To increase the control bandwidth of the FOFB system at TPS, a DFCMPS has been developed based on the architecture of the existing TPS Corrector Magnet Power Supply (CMPS). The overall system configuration is shown in Fig. 2. The power stage adopts a modular half-bridge topology, where two half-bridge modules form a full-bridge (H-bridge) structure to generate bipolar output current for the fast corrector magnets. A digital control architecture based on a Texas Instruments DSP is implemented together with analog signals conditioning circuits. The feedback current signal is digitized and processed by the DSP, where a proportional–integral (PI) compensator is used to achieve closed-loop current regulation [3].

For current feedback measurement, a high-precision DCCT is used. A LEM ITN-12-P DCCT operates in a shunt-type configuration. By modifying the primary winding turns ratio, the current measurement range is reduced from 12.5 A to 6.25 A, thereby improving the current measurement resolution and regulation accuracy.

Compared with the existing CMPS, the switching frequency of the power stage is increased from 40 kHz to 250 kHz. To support high-frequency operation, the PI control algorithm and DSP firmware are optimized to ensure that compensation calculations can be completed within each PWM interrupt cycle. In addition, conventional MOSFET devices are replaced with GaN FETs to reduce switching losses and improve high-frequency performance. The modular half-bridge design also simplifies system debugging and facilitates future upgrades of the power devices.

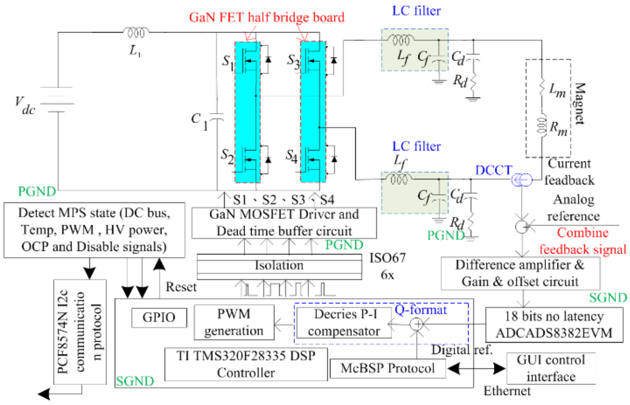

Figure 2: Architecture of DFCMPS.

GAN-BASED HALF-BRIDGE POWER STAGE DESIGN

This study investigates power converters based on GaN MOSFET switching devices. Several GaN devices with different packaging types and driving characteristics were evaluated. Corresponding isolated gate-driver circuits were designed to implement modular half-bridge power stages, enabling flexible system integration and future device replacement. The GaN MOSFET devices investigated in this work include LMG3410, LMG5200, GS61008T, and GS66508T. In the hardware implementation, two GaN FET devices together with DC bus decoupling capacitors, isolated power supplies, and digital signal isolators form a half-bridge power module. The printed circuit board (PCB) adopts a two-layer design and follows the high-speed layout guidelines provided in the device datasheets to minimize parasitic inductance and switching noise. The module dimension is 52.85 mm × 44 mm, which is defined as the standard footprint for all GaN power modules developed in this work.

Based on this standardized design, several half-bridge power modules using different GaN devices were implemented, as shown in Fig. 3, allowing flexible device selection and simplified debugging.

Figure 3: Homemade GaN FET power module.

DCCT TURNS RATIO MODIFICATION

In the original DCCT configuration, an input current range of 0 to 12.5 A generates a corresponding output signal of 0 to 50 mA. As shown in Fig. 4, after modifying the primary winding turns ratio from four to eight turns, the same 50 mA output is produced at 6.25 A, effectively doubling the current sensing sensitivity and improving the feedback resolution by a factor of two. The DCCT output current is converted into a voltage signal through a Vishay 25 Ω precision resistor with an ultra-low temperature coefficient of 1 ppm/°C, producing a 0 to 1.25 V feedback signal. This signal is then compared with the reference signal and conditioned to match the ±4.096 V input range of the ADC before entering the DSP-based control loop. As a result, the modified DCCT configuration significantly enhances the current measurement resolution and improves the accuracy of closed-loop current regulation in the DFCMPS.

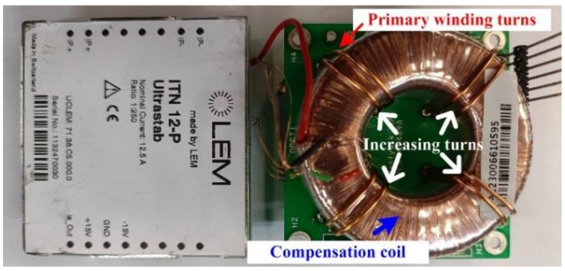

Figure 4: Adjusted DCCT turns ratio.

DSP AND Q-FORMAT COMPUTATION

To implement the current control loop, a Q-format fixed-point method was adopted for the PI compensator calculation. The PI computation is executed within the PWM interrupt service routine, where the switching frequency determines the available computation time. At a switching frequency of 40 kHz, the interrupt period is approximately 25 µs, providing about 4000 CPU clock cycles at a 150 MHz DSP clock, which is sufficient for floating-point computation. However, when the switching frequency increases to 250 kHz, the interrupt period decreases to 4 µs, leaving only about 600 CPU cycles available. Under this condition, floating-point calculations may exceed the available execution time, causing PWM update delays and resulting in unstable switching frequency.

Therefore, Q-format fixed-point computation was adopted to reduce computational complexity and CPU cycle consumption, providing sufficient processing margin for high-frequency operation. To evaluate the achievable PWM switching frequency under the implemented PI algorithm, the computational performance of the DSP was experimentally measured. As shown in Fig. 5, the DSP interrupt frequency reached 468 kHz when using Q-format computation, while PWM2 and PWM3 maintained normal modulation. In contrast, with floating-point computation, the interrupt frequency decreased to 406 kHz, and the PWM signals could not operate correctly.

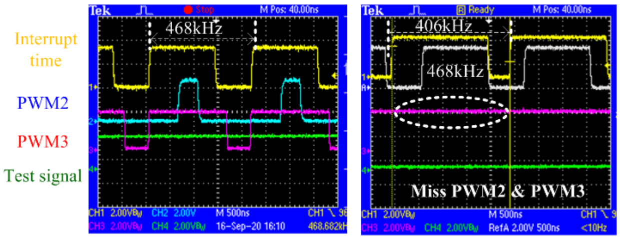

Figure 5: Timing differences in DSP algorithm.

EXPERIMENTAL RESULT

Several experiments were conducted to evaluate the performance of the proposed DFCMPS, including DSP interrupt timing measurement, step response analysis, long-term stability testing, and small-signal bandwidth characterization. To ensure measurement accuracy and reliability, high-precision instruments, including a dynamic signal analyzer (DSA) and an Ultrastab Saturn current transducer (USCT), were employed. The load used in the experiments is a TPS fast corrector air-core magnet (231.4 µH and 146.43 mΩ), providing realistic operating conditions for all performance evaluations. Fig. 6 shows the completed DFCMPS prototype developed in our laboratory. The overall hardware architecture and control interface remain fully compatible with the existing TPS CMPS system. In addition, the DFCMPS modules can be installed in a standard 19-inch rack cabinet, with up to 24 modules accommodated in a single rack, providing a compact and scalable solution for TPS FOFB applications.

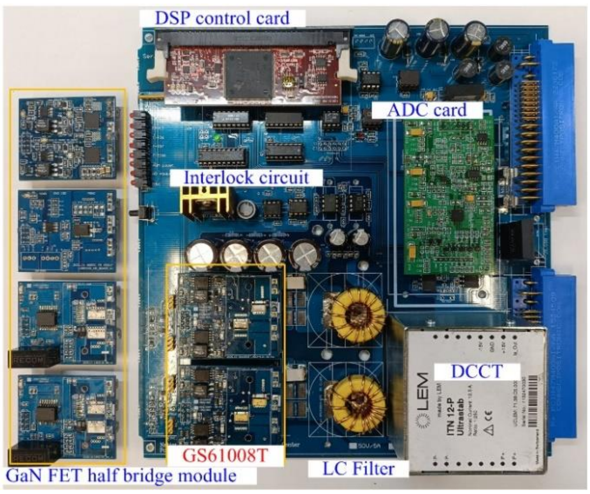

Figure 6: Hardware of the DFCMPS with GaN modules.

DSP Interrupt Execution Time

The results obtained in the previous sections confirm that the Q-format implementation significantly reduces the computational overhead of the DSP controller and provides sufficient timing margin for operation at the target switching frequency of 250 kHz. Further timing measurements performed at 250 kHz are shown in Fig. 7. The gray trace in Fig. 7 represents the interrupt execution time using floating-point computation, which is approximately 3.2 µs. In comparison, the Q-format implementation reduces the interrupt execution time by approximately 0.5 µs. Considering that the PWM period at 250 kHz is 4 µs, the Q-format method increases the available computation margin by about 12.5%, thereby improving the stability and reliability of high-frequency operation.

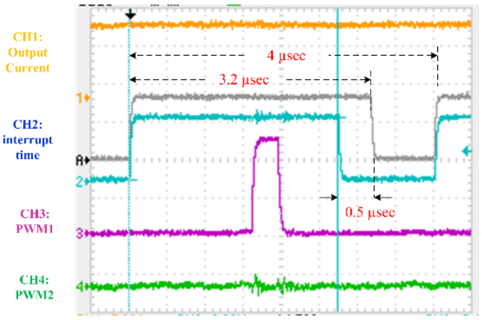

Figure 7: Relationship between algorithm and DSP computation time.

Step Response

The transient response of the DFCMPS was evaluated using a 1 V step command, as shown in Fig. 8, where the yellow line represents the reference step command. The rise time of the conventional MOSFET-based CMPS (gray line) is 150 µs, whereas the GaN FET-based DFCMPS (blue line) achieves a significantly faster rise time of less than 92 µs. This experimental result demonstrates that the proposed GaN FET system outperforms the existing 40 kHz MOSFET version and is highly suitable for fast modulation in the TPS FOFB system.

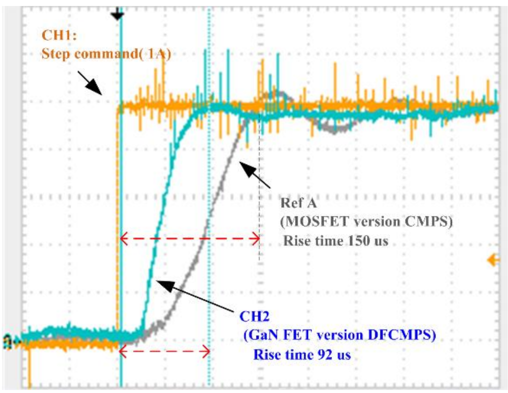

Figure 8: Step response of DFCMPS.

Stability

To minimize heat accumulation on the device surfaces during testing, heat sinks and cooling fans were installed on the GaN FET power modules of the DFCMPS. The long-term current stability of the system was evaluated using a high-precision USCT and an 8.5-digit digital voltmeter, with a TPS fast corrector magnet serving as the load. The output current was set to 5 A and recorded at 10-second intervals over an 8-hour period, as shown in Fig. 9. The measured current variation remained within 300 µA, demonstrating an exceptional stability of approximately ±30 ppm.

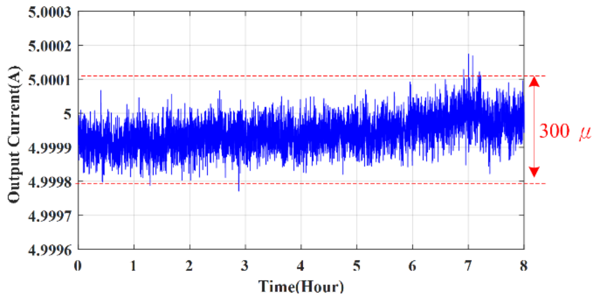

Figure 9: Output current stability of the DFCMPS.

Bandwidth

The small-signal frequency response was measured using an HP 35670A DSA with a 1 A perturbation signal. As shown in Fig. 10, the measured −3 dB bandwidth is 9.08 kHz, and the −45° phase shift occurs at 5.56 kHz. These results demonstrate that the proposed DFCMPS provides sufficient bandwidth for TPS FOFB applications.

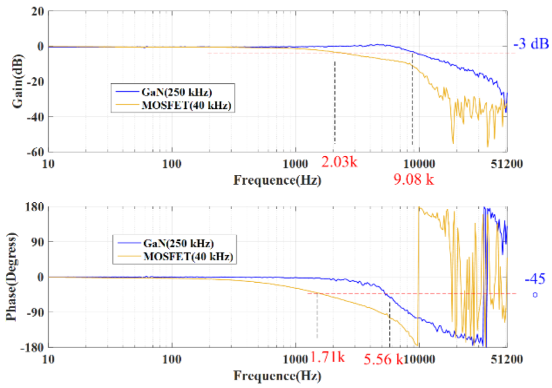

Figure 10: The bandwidth of DFCMPS.

CONCLUSION

A GaN-FET-based DFCMPS for TPS was developed to improve the bandwidth and current resolution required for FOFB operation. The design employs a modular GaN half-bridge combined into a full-bridge topology operating at 250 kHz, significantly increasing switching frequency compared with the existing 40 kHz MOSFET-based CMPS. A modified LEM ITN-12-P DCCT enhances current feedback resolution, while a DSP-based digital controller with Q-format computation ensures stable high-frequency operation.

Experimental results show a step response rise time below 100 µs, long-term current stability within ±30 ppm over 8 hours at 5 A output, and a measured small-signal bandwidth of 9.08 kHz. The proposed system demonstrates improved dynamic performance and compatibility with the existing TPS infrastructure, providing a promising solution for high-bandwidth FOFB applications in synchrotron light sources.

REFERENCES

[1] C.-C. Kuo *et al.*, "Commissioning of the Taiwan Photon Source", in *Proc. IPAC'15*, Richmond, VA, USA, May 2015, pp. 1314-1318. doi:10.18429/JACoW-IPAC2015-TUXC3

[2] K.-B. Liu, J. C. Hsu, K. T. Hsu, Y. D. Li, and B. S. Wang, "TPS Corrector Magnet Power Converter", in *Proc. IPAC'10*, Kyoto, Japan, May 2010, paper WEPD073, pp. 3269-3271.

[3] B.-S. Wang, C.-Y. Liu, K.-B. Liu, and Y. S. Wong, "Development of a GaN FETs based fully digital correction magnet power supply platform for taiwan photon source", in *Proc. IPAC'23*, Venice, Italy, May 2023, pp. 3776-3778. doi:10.18429/JACoW-IPAC2023-WEPM087